

DOI: 10.1002/cbic.201000145

Live-Cell Imaging with Water-Soluble Aminophenoxazinone Dyes Synthesised through Laccase Biocatalysis

Frédéric Bruyneel,^[a] Ludovic D'Auria,^[b] Olivier Payen,^[a] Pierre. J. Courtoy,^[b] and Jacqueline Marchand-Brynaert^{*[a]}

Aminophenoxazinone dyes with variable water solubilities were assayed for the first time in a live-cell imaging application. Among a library of ten sulfonated chromophores, one compound gave excellent results as an endocytic marker, showing a precise subcellular distribution. The compound was compared to four commercial vital tracers, including Lucifer

Yellow. The first laccase-mediated regioselective synthesis of a diphosphorylated 2-aminophenoxazinone dye was also described. This compound, water-soluble at 10^{-2} M, displayed modest fluorescence properties and the ability to complex Mg^{2+} and Ca^{2+} cations, therefore giving fluorescence quenching.

Introduction

Fluorescent organic dyes are widely used as markers in the field of molecular biology and biomedical research.^[1,2] Such nonradioactive probes allow the labelling of biomolecules that are of interest for imaging cell structure and function.^[3,4] Indeed, the subcellular distribution, physical association and specific interactions of biological molecules at, and inside the cell are of central importance. All of these aspects are particularly relevant to the study of the growing number of human disorders that are related to a defect in the endo-lysosomal system.^[5] Moreover, metabolic mapping in living cells encompasses a large set of cellular events, among which endocytic pathways remain an important research field.^[6,7] In practice, live-cell imaging with endocytic markers is usually explored among the first potential applications whenever one desires to develop a new class of fluorophores for molecular biology. On the other hand, whereas numerous available synthetic fluorescent dyes exhibit high quantum yields, narrow emission bands up to the near-infrared and good photostability, the severe drawback of poor water solubility decreases the utility of most of them.^[1] Commonly, improved water solubility is obtained through the insertion of ionisable hydrophilic groups into the fluorophore core structure, or by dye conjugation to biopolymers such as carbohydrates.^[8,9] In the former strategy, functions such as sulfonic, and/or ammonium groups are the most popular ones, and have been widely used in the case of benzo[a]phenoxazine and xanthene dyes, thus leading to several families of water-soluble fluorophores endowed with high quantum yields.^[10,11] The classical synthetic pathway towards benzo[a]phenoxazine dyes involves a nitrosative condensation that is poorly efficient with sulfonated building blocks.^[12] This only improves solubility at the last stage of the chemical synthesis, and thus considerably limits the diversity of novel probe libraries.

Aminophenoxazinone dyes and pigments have been known for several decades, most of them being of natural sources.^[13] Their potential use as fluorescent probes has been mainly pre-

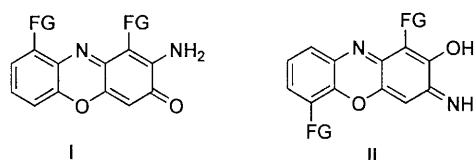
vented by low water solubility and the absence of a general methodology for the production of diversely substituted phenoxazinone scaffolds.^[14] Recently, our group reported a novel synthetic approach, based on the use of laccase as a biocatalyst, which showed promising results for the "green" production of phenoxazinone dyes featuring variable water solubility.^[15] From a pool of diverse benzenesulfonyl derivatives as substrates, the last synthetic step corresponds to a cyclising oxidative dimerisation conveniently performed at room temperature, in aqueous solution, and with air as oxidant.

Herein, we report an extension of this methodology by the production of the first phosphorylated aminophenoxazinone dye. This water-soluble compound, along with the previously prepared series of sulfonated phenoxazinone dyes (see Scheme 1 for general core structures) were further studied for their optical properties and screened for their potential in fluorescence live-cell imaging. The best candidate (compound **8c**) was finally characterised as an endocytic tracer of the degradative pathway, by reference to known fluorescent probes targeted to endosomes, lysosomes or the Golgi complex, by using double-labelling experiments.

[a] Dr. F. Bruyneel, Dr. O. Payen, Prof. Dr. J. Marchand-Brynaert
Institute of Condensed Matter and Nanosciences (IMCN)
Organic and Medicinal Chemistry Unit (CHOM)
Université catholique de Louvain
Bâtiment Lavoisier, Place Louis Pasteur 1, 1348 Louvain-la-Neuve (Belgium)
Fax: (+32) 10-474168
E-mail: jacqueline.marchand@uclouvain.be

[b] L. D'Auria, Prof. Dr. P. J. Courtoy
Cell Biology unit (CELL) and Platform for Imaging Cells and Tissues (PICT)
de Duve Institute (ICP-UCL-7541), Université catholique de Louvain
75, avenue Hippocrate, 1200 Bruxelles (Belgium)

Supporting information for this article is available on the WWW under <http://dx.doi.org/10.1002/cbic.201000145>.

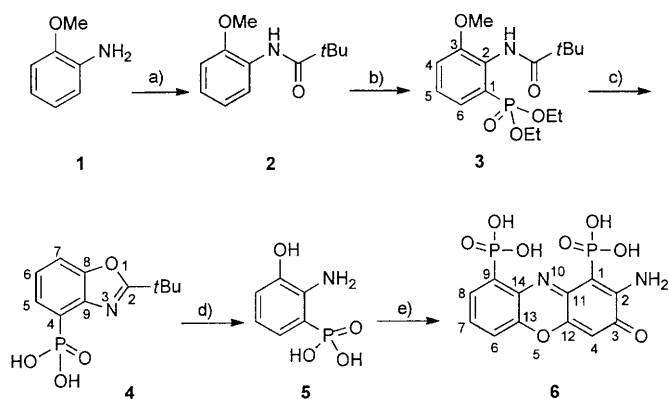


Scheme 1. General structures (I) and (II) of studied fluorescent dyes. FG = functional group responsible for the solubility properties.

Results and Discussion

Chemistry

From a synthetic point of view, the Michaelis–Arbuzov reaction was the traditional method employed when phosphorylated aromatic dyes had to be produced.^[16] However, this strategy implies the regioselective synthesis of aromatic halides as starting materials. The directed-metallation reaction has proven to be an alternative method of choice to insert selectively an oxidised phosphorous group in organometallic chemistry.^[17] Based on a synthetic approach previously used by our group for selective aromatic sulfonation, we have taken advantage of the insertion of a lithiated intermediate into a P–Cl bond, which leads to the corresponding phosphorylated precursor in good yield and complete selectivity. Next, a laccase was used as catalyst to promote the oxidative cyclisation of the substrate into the first diphosphorylated 2-aminophenoxazinone dye produced as a single regioisomer. The synthetic pathways for the efficient synthesis of our phosphorylated building block and its dimerisation are outlined in Scheme 2.



Scheme 2. Synthesis of aminophenoxazinone **6**. Reagents and conditions: a) 1.1 equiv *t*BuCOCl, 3 equiv NaHCO₃, H₂O/EtOAc, 25 °C, 4 h; b) 2.4 equiv *n*BuLi, 2.4 equiv TMEDA, THF, 2.4 equiv (EtO)₂POCl, –10 °C, 2 h, then overnight at 25 °C; c) 3 equiv BBr₃, CH₂Cl₂, 0 °C, 2 h, then 25 °C, 18 h; d) HCl (12 N), 100 °C, 24 h; e) MeOH/NH₄OAc (0.2 M, pH 6), laccase 100 U L⁻¹, air, 25 °C, 24 h.

Briefly, commercially available *o*-anisidine (**1**) was quantitatively protected (step a) as *N*-pivaloyl derivative (**2**). The crude intermediate was submitted to regioselective lithiation because of the slight difference in directing ability in favour of the *N*-pivaloyl function over the *O*-methyl ether. By using 2.4 equivalents of *n*BuLi in the presence of tetramethylethylenediamine (TMEDA) as activating agent, the lithiated aromatic

intermediate was produced in situ and then treated with 2.4 equivalents of diethyl chlorophosphate (step b) to give compound **3** in 70% yield after chromatography. Next the methyl ether function was cleaved using an excess of boron reagent in dichloromethane (step c). After usual work-up and precipitation in diethyl ether, pure benzoxazole compound **4** was obtained in 78% yield. Interestingly, spontaneous intramolecular cyclisation was observed here, in the same way as previously described for the sulfonated analogue.^[15a] This original 2-*tert*-butyl-4-phosphonic acid benzoxazole was hydrolysed in a 12 N HCl solution at reflux (step d) to give the precursor **5** as a white powder in 70% yield, after concentration and precipitation.

To date, there is no example of a laccase-mediated oxidative coupling reaction that makes use of organic phosphorylated compounds as substrates. Sulfonic and phosphonic groups being considered as bioisosteres of the carboxylic function,^[18] the previous conditions of our laccase-catalysed synthesis in water were applied to compound **5**. In the presence of a catalytic amount of laccase in an aqueous buffer at pH 6, substrate **5** was converted at room temperature (step e) into the corresponding 1,9-disubstituted phenoxazinone dye **6** as a >95% pure compound with an excellent yield of 90% after isolation. Briefly, the reaction was monitored by HPLC until complete conversion of **5**; next the laccase was inactivated by adding 40% (v/v) of methanol, and concentrated in vacuo before freeze-drying of the remaining solution. The residual red powder was fully characterised by HRMS and IR, NMR (¹H and ¹³C) and UV–visible spectroscopy. The novel bis-phosphorylated dye **6** is highly water-soluble: solutions of **6** up to a concentration of 10⁻² M can be prepared in PBS or pure water. In methanol, the highest concentration reached is about 5 × 10⁻⁴ M. Syntheses and structural elucidations of the related bis-sulfonylated dye **7** and derivatives **8 a–g** and **9** (see Table 1) were previously reported.^[15b]

Table 1. UV/Vis absorption data of dyes **6–9**.^[a]

Compound	Functional group ^[b]	Core ^[b]	$\epsilon \times 10^3$ [M ⁻¹ cm ⁻¹]	λ_{\max} [nm] ^[c]
6	PO ₃ H	I	8.80	241, <u>438</u>
7	SO ₃ H	I	9.80	240, 418, <u>441</u>
8 a	SO ₂ NH ₂	I	4.04	240, 436, <u>451</u>
8 b	SO ₂ NH-cyclohexyl	I	10.80	236, 424, <u>456</u>
8 c	SO ₂ NH(CH ₂) ₃ N(Me) ₂	I	7.20	239, 422, <u>442</u>
8 d	SO ₂ NH-phenyl	I	0.48	240, <u>430</u>
8 e	SO ₂ NH(CH ₂) ₂ NH ₂	I	6.02	240, 423, <u>442</u>
8 f	SO ₂ NHCH ₂ CO ₂ Me	I	5.90	238, 422, <u>442</u>
8 g	SO ₂ NH(CH ₂) ₂ CH ₂ OH	I	12.60	240, 420, <u>440</u>
9	SO ₂ NH-cyclohexyl	II	3.95	238, 420, <u>430</u>

[a] Measured in PBS at pH value of 7.4. [b] See Figure 1. [c] The underlined value corresponds to the given ϵ (molar coefficient extinction).

Absorption and fluorescence properties

The photophysical properties of the aminophenoxazinone dyes featuring variable water solubilities were evaluated under simulated physiological conditions, that is, in phosphate-buffered-saline solution (PBS; 0.15 M) at pH 7.4. The UV–visible

spectra of compounds **6–9** showed absorptions between 420 and 450 nm with ϵ values ranging from 480 to $12\,600\text{ M}^{-1}\text{ cm}^{-1}$ (Table 1 and Scheme 1). Data collections were performed at concentrations ranging from 5×10^{-4} to $1 \times 10^{-6}\text{ M}$ to ensure full solubility of all compounds. Rather low ϵ values were obtained for dyes **8a**, **8d** and **9**, whereas the ϵ values for **8c**, **8e** and **8f** were slightly higher. The highest ϵ values were recorded for the dyes **6**, **7**, **8b** and **8g**. Still, the absorbance of these newly synthesised compounds was ten- to 100-fold lower than for a classical benzo[a]phenoxazinone dye ($\epsilon = 42.4 \times 10^3\text{ M}^{-1}\text{ cm}^{-1}$).^[10a]

Next, the fluorescence properties of the functionalised aminophenoxazinone dyes **6–9** were evaluated at concentrations ranging from 5×10^{-5} to $1 \times 10^{-4}\text{ M}$ by using rhodamine 6g (Rho-6g) as reference (Φ_F (quantum yield) = 0.95, see the Supporting Information); the results are summarised in Table 2.

Compound	λ_{exc} [nm]	λ_{em} [nm]	Φ_F	Stokes' shift [nm]
6	488	500–650	0.003	110
7	488	500–600	0.001	~100
8a	488	520–680	0.009	122
8b	488	520–680	0.007	130
8c	488	500–700	0.017	116
8d	488	570–620	0.0004	~100
8e	488	500–700	0.007	146
8f	488	500–700	0.014	146
8g	488	500–700	0.005	~130
9	488	520–650	0.002	~100

[a] Measured in PBS (0.15 M) at pH value of 7.4.

Dye concentrations were adjusted to yield an identical optical density of 0.06 in PBS (0.15 M). Emission spectra after excitation at $\lambda = 488\text{ nm}$ were recorded between 500 and 700 nm. All dyes exhibited some fluorescence, albeit with a rather low intensity. Clear emission maxima were observed around 560 nm, while some dyes, such as **7**, **8d**, **8g** and **9**, emitted broadly from 500 to 650 nm without clear maxima. Relative quantum yields measured by reference to Rho-6g were in general rather low, almost 100 times lower than that of Lucifer Yellow (LY; $\Phi_F = 0.21$, see the Supporting Information).^[19] Two dyes, **8c** and **8f**, emerged as most promising based on this criterion, with quantum yields close to 0.02. Dyes **6**, **8a–c** and **8e** exhibited a large Stokes' shift ranging from 110 to almost 150 nm depending on the functional groups inserted in the core structures (see Figure 1). Compounds bearing sulfonated side chains were always more efficient than the parent sulfonic acid **7**, whereas compound **6**, bearing free phosphonic acids, still gave a quite significant Stokes' shift. Hydrophobicity did not seem to play a major role either. Whereas dyes **6** and **7** exhibited similar molar extinction coefficients, a puzzling difference in emission spectra was observed.

Although it was the first time that such heterocyclic chromophores became available for testing in biological media, it might seem brave to apply dyes **6–9** in fluorescence labelling experiments, given their rather limited quantum yield. Never-

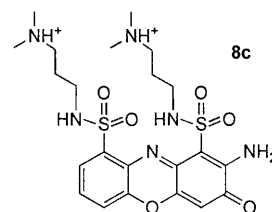
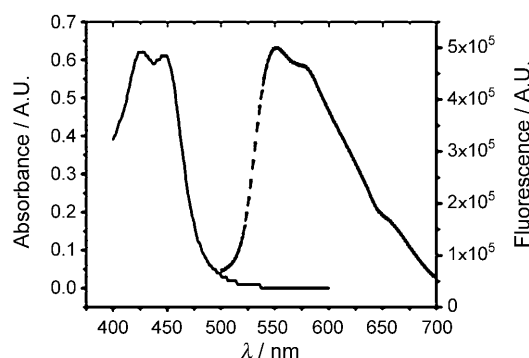


Figure 1. Absorption (solid line, left axis) and fluorescence (dashed line, right axis) spectra of $5 \times 10^{-5}\text{ M}$ **8c** in PBS at pH 7.4. A.U. = arbitrary unit of fluorescence.

theless, a first screen by live-cell imaging was undertaken using CHO (Chinese Hamster Ovary) cells after 1 hour of incubation at 37°C with the entire series of phenoxazinone dyes at 1 mg mL^{-1} , with the exception of compound **8d**. The results of this visual screen are summarised in Table 3. It immediately ap-

Compound	Fluorescence	Location	Aggregate	Cell state ^[b]
6	null	–	–	–
7	low	–	–	good
8a	low	intracellular	–	good
8b	high	extracellular	massive	stressed
8c	medium	intracellular	–	good
8e	low	intracellular	small	good
8f	medium	intracellular	–	good
8g	medium	intracellular	–	good
9	null	extracellular	massive	stressed

[a] Excitation at 488 nm, Emission filter at 526–532 nm. Transmission at 5%; detection in the green channel. [b] Stress was attributed to aggregation. Due to the variable water solubility of dyes, final concentrations of ethanol in this preliminary screen ranged from 0.5 to 5% for **8a**, **b**, **e**, **f**, **g**, and **9**, and were below 0.5% for **6**, **7** and **8c**.

peared that the significant hydrophobicity of compounds **8b** and **9** caused massive aggregation, therefore preventing any application to biological systems. Overall, the cell did not appear to be appreciably altered, despite the rather high final ethanol concentration in this screen.

The candidate selected for further imaging was the water-soluble compound **8c**, which also offers the highest quantum yield. Furthermore, its intracellular distribution in well-defined spots readily pointed to its potential as an endocytic tracer.

The puzzling result observed with compound **6** seemed, a priori, quite disappointing. Such an absence of fluorescence, when even compound **7** could be detected in the experiments, led us to consider that the data obtained with compound **6** were the result of an artefact. Bearing in mind the well-known ability of phosphonate groups to chelate divalent cations, we envisaged a quenching of fluorescence due to the presence of Mg^{2+} and Ca^{2+} ions in the culture medium of CHO cells. Such a loss of fluorescence due to the chelation of Mg^{2+} and/or Ca^{2+} was indeed confirmed independently (Supporting Information). Whereas compound **6** (4.6 mM) fluoresced in pure water and PBS (0.15 M NaCl, 0.8 mM PO_4^{2-}), the quenching was complete in the presence of PBS doped with Ca^{2+}/Mg^{2+} (3 mM each) and similarly in aqueous solutions of each cation (3 mM).

Subcellular localisation of compound **8c**

Several endocytic pathways, all based on pinching-off vesicles from the plasma membrane invaginations, allow bulk or selective internalisation of extracellular, membrane impermeant compounds.^[5] Bulk (i.e., fluid-phase or nonspecific adsorptive) endocytosis allows us simultaneously to explore the various internalisation portals and intracellular endocytic routes.^[7] The *endo*-lysosomal system comprises early, sorting, late and recycling endosomes, secondary lysosomes and the trans-Golgi network. Although early endosomes are primarily involved in sorting internalised compounds and membrane, recycling endosomes ensure the homeostasis of the plasma membrane.^[22] Lysosomes are usually the final destination where internalised macromolecules are to be degraded. A large variety of fluorescent probes are available to analyse this complex system.^[20–23] Some of these, such as LY, are widely used as tracers for fluid-phase endocytosis.^[24] Other fluorescent dyes have shown intrinsic properties that permit the selective labelling of well-defined intracellular compartments, such as the recycling pathway (transferrin),^[23] lysosomes^[24] or the Golgi complex (BODIPY-ceramide).^[25]

To rule out diffusion as a mechanism contributing to intracellular labelling by compound **8c**, two classical endocytic controls were carried out: energy depletion and low-temperature block. As illustrated in Figure 2, cells incubated with 1.5 mM of compound **8c** for 45 min in serum-free medium showed multiple intracellular dots, with preferential clustering around the nucleus. In contrast, ATP-depleted cells exposed to compound **8c** at 37 °C, or untreated cells incubated with this compound at 4 °C showed no fluorescence. The integrity of the plasma membrane was verified by simultaneous labelling with CellTracker Red, a fluorescent membrane-permeant probe that becomes membrane-impermeant after conjugation with glutathione (see the Supporting Information for chemical structures).

We next analysed the fate of internalised compound **8c**, by reference to the vital tracers of recycling endosomes (Alexa 568-transferrin), the Golgi complex (BODIPY-ceramide, a metabolic precursor of BODIPY-sphingomyelin), and LysoTracker Red, which, like chloroquine and acridine orange, are mem-

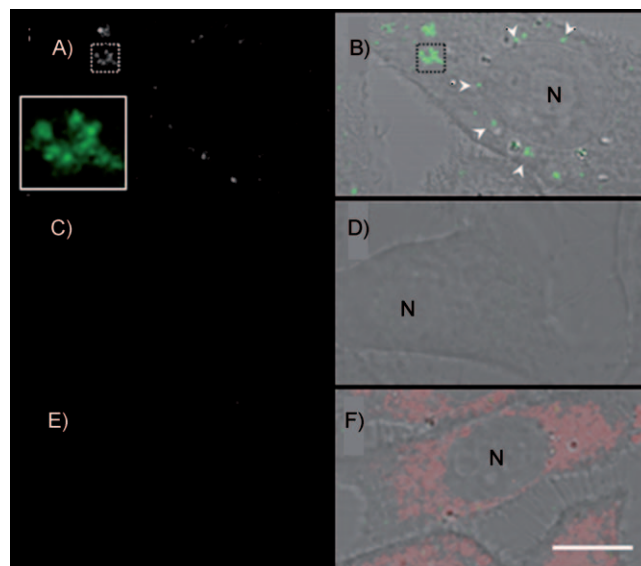


Figure 2. Evidence for endocytic uptake of compound **8c**. A), B), E), F) Control or C), D) ATP-depleted CHO cells were incubated for 45 min with 1.5 mM of compound **8c** at 37 °C in A), B) control or C), D) ATP-depleting medium; or E), F) at 4 °C in the presence of 10 μ M CellTracker, for global cell imaging. The figure shows dark-field fluorescent images (left), merged with transmission images (right). In the upper panel, control cells showed bright intracellular punctate labelling, mainly perinuclear (arrowheads). The boxed area at A) is enlarged in the inset. As shown by the central and lower panels, ATP-depletion (C, D) or incubation at 4 °C (E, F) does not lead to green intracellular labelling. In (F), the integrity of the plasma membrane is demonstrated by cytosolic labelling with CellTracker Red. These experiments demonstrate that **8c** accumulates in cells by a temperature and energy-dependent mechanism that is consistent with endocytosis. N = nucleus, scale bar = 10 μ m.

brane-permeant in their nonprotonated form and become sequestered upon protonation in acidified, closed compartments. As shown in Figure 3, compound **8c** fully segregated from recycling endosomes and the Golgi complex, and was exclusively targeted to late endosomes/lysosomes.

Finally, to test whether compound **8c** qualified as a bulk endocytic tracer, its endocytic trafficking was compared with that

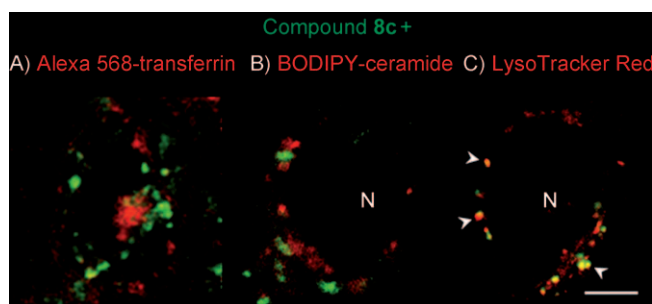


Figure 3. Internalised compound **8c** is targeted to late endosomes/lysosomes. CHO cells were incubated with **8c** at 37 °C for 45 min together with A) (in red) 0.7 μ M Alexa 568-transferrin (tracer of recycling endosomes), B) 5 μ M BODIPY-ceramide (a vital stain of the Golgi complex) or C) 50 nM LysoTracker (to label late endosomes/lysosomes by acidotropic sequestration). Note that internalised **8c** fully segregates from recycling endosomes and the Golgi complex and is exclusively targeted to late compartments of the degradative pathway. N = nucleus, scale bar = 10 μ m.

of LY, as illustrated in Figure 4. Interestingly, although compound **8c** is a cationic species, due to protonation of its tertiary amino groups, and the bisulfonate compound LY is an anionic species, both endocytic tracers labelled similar structures and apparently progressed towards lysosomes at a comparable rate.

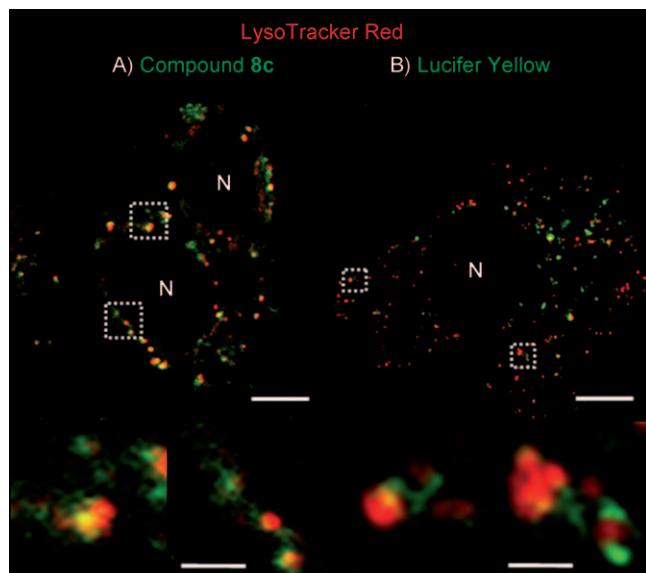


Figure 4. Despite bearing opposite net charges, compound **8c** and Lucifer Yellow are expected to follow late endosomes/lysosomes by default. CHO cells were incubated at 37 °C for 45 min with 50 nM LysoTracker Red together with 1.5 mM compound **8c** (left) or 2.2 mM LY (right), and then briefly washed and studied by live confocal microscopy. Optical sections at the level of the nucleus (N) are shown. The boxed areas, enlarged tenfold below, suggest that pleiomorphic late endosomes, filled by endocytosis of the membrane-impermeant tracers, **8c** or LY, dock with lysosomes concomitantly labelled by acidotropic sequestration of the membrane-permeant probe, LysoTracker Red. Scale bars: upper panel 10 μm, lower panel 1 μm.

Conclusions

We here provide the first report on a series of water-soluble aminophenoxazinone dyes that have been evaluated for vital imaging in cell biology. These heterocyclic compounds were produced by using an enzymatic synthetic strategy, as an alternative to the nitrosative or chemical oxidative coupling of phenolic precursors. Thus, the first 1,9-bis-phosphorylated aminophenoxazinone dye (**6**) has been synthesised in excellent yield by taking advantage of laccase-mediated oxidation in water. The fluorescence quenching observed when **6** was mixed with Mg^{2+} and/or Ca^{2+} brought about a heavy handicap in the cell labelling application, but could lead to its development as a sensor for variations in divalent cation concentrations in the high range. Among the first generation of tested dyes, namely the sulfonylated compounds **7–9**, one dye, **8c**, appears particularly promising as a presumably bulk endocytic tracer with targeting by default to lysosomes. Despite having a tenfold lower quantum yield than Lucifer Yellow, compound **8c** generated intracellular signals of comparable intensity. However, it remains to be tested whether this useful “compensation” for

an endocytic tracer could be ascribed to the benefit of membrane adsorption, due to charge complementarity with the cell surface glycocalyx. While the other sulfonylated water-soluble chromophores **7–9** suffer from much lower quantum yields, they might eventually reveal interesting properties yet to be explored. Finally, dyes **8e–g** feature at least one free reactive function for further conjugation to biomolecules and grafting to materials, which opens the route towards selective labelling experiments.^[26]

Experimental Section

General methods: 1H , ^{13}C and ^{31}P NMR spectra were recorded with a Bruker Avance 500 or a Bruker Avance 300 spectrometer. Spectra were obtained in $[D_6]DMSO$, $CDCl_3$, D_2O or CD_3OD . Chemical shifts are reported in ppm relative to tetramethylsilane.^[27] ^{13}C NMR spectra were obtained with broadband proton decoupling ($D1 = 5$ s) or DEPTQ. Low-resolution mass spectra were acquired on a Thermo Finnigan LCQ spectrometer, either in positive- or negative-mode ESI. HRMS analyses by using ESI or FAB methods were performed at the University of Mons Hainaut (Belgium) or at the University of Oxford (UK). Melting points were recorded with an Electrothermal apparatus calibrated with benzoic acid. Infrared spectra were recorded with a Shimadzu FTIR 84005 spectrometer using KBr plates. The HPLC system consisted of a Waters Alliance 2699 separation module, and a Waters 2998 photodiode array detector; analytical separations were performed on a Waters XterraMSC18 column (4.6 mm × 100 mm, 5 μm; Waters, Milford, MA, USA) equipped with a conventional precolumn. Detection was performed at 220/254/280 nm with a control at 440/460 nm and on-line UV/Vis absorbance scans were performed. Flow rate was 1 mL min⁻¹. Initial conditions were ACN 100% for 5 min, then a hyperbolic gradient to 75:25 of solvents A (water/HCO₂H, 100:0.1 v/v) and B (ACN/HCO₂H, 100:0.1 v/v) over 5 min, then a hyperbolic gradient to 25:75 of A/B in 10 min. Then, the cycle was terminated by returning to the initial conditions over 5 min. The injection volume was 10 μL.

Materials: Lucifer Yellow (LY) was purchased from Sigma. Other commercial fluorescent probes, namely Tfn-Alexa 568, ceramide-BODIPY-589, Cell-Tracker-Red and LysoTracker-Red were obtained from Invitrogen. Laccase from *Trametes versicolor* was purchased as a brownish powder from Bioscreen e.K. (Uebach-Palenberg, Germany) under the commercial trademark Oxizym LA (batch no. LA 2000/001).

Fluorescence measurements: UV/Vis spectra were recorded on a UV/Vis–NIR Varian-CARY spectrophotometer (λ given in nm). Emission fluorescence spectra were recorded on a Fluorolog-3 spectrofluorometer (Jobin Yvon Horiba). The excitation spectra (emission at 500–700 nm, window of 526–534 nm used for Φ_F) and emission spectra (excitation at 488 nm) of aminophenoxazinone dyes were determined in PBS (pH 7.4) over a range of concentrations around 10⁻⁵ M (optical density of 0.06). The ϵ values were also obtained in phosphate-buffered solutions. The fluorescence intensities in pure water were measured from the corrected emission curve by using the area function of the fluorometer. Relative fluorescence quantum yields were obtained by using Rho-6g ($\Phi_F = 0.95$) as the reference.

Quenching of fluorescence: Fluorescence experiments of dyes **6**, **7**, **8a**, **8e** and **8g** in the presence of Mg^{2+} (3 mM) and/or Ca^{2+} (3.6 mM) either in PBS or pure water were realised in triplicate in a 96-well plate. Fluorescence was recorded by using a HP Fluorocount mounted with an excitation filter at 488 nm and an emission

filter at 530 nm. Blanks were recorded with and without dyes in PBS or water. A quenching phenomenon was observed only for dye 6.

Cell culture and labelling: CHO cells were propagated in DMEM/F-12 supplemented by 10% foetal calf serum and antibiotics.^[28] For experiments, cells were seeded at ~20 000 cm² on Lab-Tek chambers (Nunc, Roskilde, Denmark) and grown until ~90% confluency (2 days). For the primary screening, probes were dissolved in ethanol (20 mg mL⁻¹), then diluted to 1 mg mL⁻¹ in PBS. For the analysis of the subcellular localisation of dye **8c**, this probe was dissolved from a stock solution in ethanol (200 mg mL⁻¹) into DMEM containing defatted BSA (1 mg mL⁻¹) to prevent adsorption to the culture vessel, to a final concentration of 1 mg mL⁻¹ (1.5 mM). For comparative studies with LY, both compounds were added to 0.5% ethanol, (final concentration).

Live-cell imaging by confocal microscopy: Extensively washed cells were examined under a Zeiss LSM510 confocal microscope equipped with an incubation chamber set at 37 °C (Zeiss; Incubator XL/LSM) and a 63× immersion oil, NA 1.4 objective. Images were recorded sequentially in the green, and then the red channels. For commercial probes, the laser was set at 2–5% (detector gain, 700; amplifier offset, -0.5). For aminophenoxazinone probes the laser was set at 4–8% (detector gain, 750; amplifier offset, -0.5).

Organic synthesis

N-(2-Methoxy-phenyl)-2,2-dimethyl-propionamide (2): NaHCO₃ (11.17 g, 3.0 equiv) and pivaloyl chloride (6 mL, 1.1 equiv) were added to a solution of *o*-anisidine **1** (5.46 g, 5.00 mmol) in ethyl acetate/water (130:150 mL). The solution was stirred at room temperature for 6 h. The layers were separated, and the organic layer was washed with aqueous 1 N HCl. The organic layer was dried over MgSO₄ and evaporated. The title compound was obtained in a quantitative yield (10.86 g). ¹H NMR (300 MHz, CDCl₃): δ = 1.31 (s, 9H; tBu), 3.87 (s, 3H; OCH₃), 6.85 (dd, ³J(H-H) = 7.9 Hz, ⁴J(H-H) = 1.8 Hz, 1H; H₆), 6.94 (td, ³J(H-H) = 7.6 Hz, ⁴J(H-H) = 1.8 Hz, 1H; H₄), 7.01 (td, ³J(H-H) = 7.9 Hz, ⁴J(H-H) = 1.8 Hz, 1H; H₅), 8.13 (s, 1H; NH amide), 8.41 ppm (dd, ³J(H-H) = 7.6 Hz, ⁴J(H-H) = 1.8 Hz, 1H; H₃); ¹³C NMR (75 MHz; [D]CDCl₃): δ = 27.6 (C(CH₃)₃), 40.0 (C(CH₃)₃), 55.8 (OCH₃), 109.8 (C6), 119.5 (C3), 121.1 (C4), 123.4 (C5), 127.9 (C2), 148.0 (C1), 176.5 ppm (CO amide).

1-Diethoxyphosphoryl-2-(2,2-dimethyl-propionylamino)-3-methoxybenzene (3): The glassware was flame-dried under argon. TMEDA (6.95 mL, 2.4 equiv) and a solution of *n*BuLi in hexane (2.5 mL, 18.5 mL, 2.4 equiv) were added dropwise to a solution of **2** (4 g, 19.30 mmol) in anhydrous THF (40 mL) at -10 °C. The addition lasted for 5 min. The mixture was stirred at -10 °C for 15 min, then at room temperature for 3 h. At -10 °C, diethylchlorophosphate (6.72 mL, 2.4 equiv) was added dropwise to the solution. The reaction mixture was stirred at -10 °C for 2 h, then warmed to room temperature over 17 h. An aqueous solution of 1 N HCl was added and the mixture was extracted with ethyl acetate. The organic phase was washed with water, dried over MgSO₄ and evaporated. The red oil (7.92 g) was purified by column chromatography on flash silica gel (eluent: cyclohexane/ethyl acetate 1:1, then ethyl acetate); two fractions were obtained. The first one was an orange oil corresponding to the starting compound **2** (0.72 g; recovery = 18.2%; conversion = 81.8%). The second fraction was a yellow solid corresponding to the title compound **3** (4.56 g; yield = 68.9%). ¹H NMR (300 MHz; CD₃OD): δ = 1.30 (m, 6H; PO(CH₂CH₃)₂), 1.32 (s, 9H; tBu), 3.83 (s, 3H; OCH₃), 3.99–4.12 (m, 4H; PO(CH₂CH₃)₂), 7.31–7.36 (m, 1H; H₃), 7.41–7.46 ppm (m, 2H; H₄ and H₅); ¹³C NMR

(75 MHz; CDCl₃): δ = 16.3 (d, ⁴J(C-P) = 6.8 Hz, PO(CH₂CH₃)₂), 27.6 (C(CH₃)₃), 39.8 (C(CH₃)₃), 56.3 (OCH₃), 63.6 (d, ³J(C-P) = 5.3 Hz, PO(CH₂CH₃)₂), 117.7 (d, ⁴J(C-P) = 2.6 Hz, C4), 124.2 (d, ¹J(C-P) = 182.0 Hz, C1), 124.4 (d, ²J(C-P) = 6.8 Hz, C6), 127.2 (d, ³J(C-P) = 16.8 Hz, C5), 129.4 (d, ²J(C-P) = 6.1 Hz, C2), 155.4 (d, ³J(C-P) = 16.2 Hz, C3), 176.6 ppm (CO amide); ³¹P NMR (121 MHz; CD₃OD): δ = 18.55 ppm (s, PO(OEt)₂); MS (ESI) *m/z* (%): 344.18 (100) [M+H]⁺; HRMS (ESI): calcd for C₁₆H₂₆NO₅NaP: 366.1446, found: 366.1434.

2-tert-Butylbenzoxazole-4-phosphonic acid (4): The glassware was flame-dried under argon. A solution of BBr₃ in dichloromethane (1 M, 18.63 mL, 3.0 equiv) was added dropwise to a solution of compound **3** (2.132 g; 6.21 mmol) in anhydrous dichloromethane (70 mL) at 0 °C. The mixture was stirred at 0 °C for 1 h, then at room temperature for 18 h. The mixture was cooled to 0 °C, and water was added dropwise to quench the residual BBr₃. The solution was evaporated, and the residue was filtered on RP-18 silica gel with methanol/water (1:1), then methanol. After evaporation, both residues were dissolved several times in diethyl ether; each time, the formed white solid was filtered and dried. The title compound was isolated with an overall yield of 77.9% (1.234 g). M.p. 204–207 °C; ¹H NMR (300 MHz; CD₃OD): δ = 1.51 (s, 9H; tBu), 7.41 (td, ³J(H-H) = 7.8 Hz, ⁴J(H-P) = 3.2 Hz, 1H; H₆), 7.74 (d, ³J(H-H) = 7.7 Hz, 1H; H₇), 7.79 ppm (dd, ³J(H-H) = 7.50 Hz, ⁴J(H-P) = 14.3 Hz, 1H; H₅); ¹³C NMR (75 MHz; CD₃OD): δ = 28.7 (tBu), 35.4 (C-(CH₃)₃), 115.0 (C7), 124.4 (d, ¹J(C-P) = 185.8 Hz, C4), 125.2 (d, ³J(C-P) = 14.6 Hz, C6), 128.8 (d, ²J(C-P) = 7.8 Hz, C5), 143.2 (d, ²J(C-P) = 6.7 Hz, C9), 152.5 (d, ³J(C-P) = 15.2 Hz, C8), 175.7 ppm (C2); ³¹P NMR (121 MHz; CD₃OD): δ = 11.02 ppm (s, PO(OH)₂); MS (ESI): *m/z* (%): 256.18 (100) [M+H]⁺; HRMS (ESI): calcd for C₁₁H₁₃NO₄P: 256.0739, found 256.0736.

2-Amino-3-hydroxy-benzenephosphoric acid (5): A solution of **4** (0.410 g; 1.61 mmol) in HCl (12 N, 20 mL) was heated at 100 °C for 24 h. The reaction mixture was cooled down to room temperature and evaporated. The residue was added with water, and the remaining solid was dissolved in methanol/diethyl ether. After evaporation under vacuum, the title compound was obtained as a white solid (0.21 g) with a yield of 69%. M.p. 202–206 °C; ¹H NMR (300 MHz; [D₆]DMSO): δ = 6.42 (td, ³J(H-H) = 7.6 Hz, ⁴J(H-P) = 4.08 Hz, 1H; H₅), 6.74 (dd, ³J(H-H) = 7.41 Hz, ⁴J(H-H) = 1.2 Hz, 1H; H₄), 6.88 ppm (ddd, ³J(H-H) = 7.6 Hz, ⁴J(H-H) = 1.2 Hz, ³J(H-P) = 12.1 Hz, 1H; H₆); ¹³C NMR (75 MHz; [D₆]DMSO): δ = 115.1 (d, ¹J(C-P) = 177 Hz, C1), 116.1 (d, ³J(C-P) = 14.7 Hz, C5), 116.2 (C4), 122.7 (d, ²J(C-P) = 6.9 Hz, C6), 138 (d, ²J(C-P) = 8.5 Hz, C2), 144.6 ppm (d, ³J(C-P) = 16.5 Hz, C3); ³¹P NMR (121 MHz; [D₆]DMSO): δ = 15.87 ppm (s, PO(OH)₂); MS (ESI) *m/z* (%): 190.14 (100) [M+H]⁺; HRMS (ESI): calcd for C₆H₉NO₄P: 190.0269, found 190.0273.

2-Amino-3-oxo-3H-phenoxazine-1,9-diphosphonic acid (6): A solution of **5** (0.2 g, 1.06 mmol) in MeOH (25 mL) was diluted to a final volume of 500 mL with water (220 mL) and ammonium acetate buffer (250 mL, 0.2 mM, pH 6). The reaction was started by adding a solution of laccase (5 mL, 10⁴ U L⁻¹), and the stirred mixture was kept for 24 h at 25 °C under air. The reaction was stopped by adding 40% (v/v) of methanol and concentrated under vacuum to a volume of 300 mL. The crude mixture was freeze-dried to give a red powder (0.2 g) with a yield of 90%. The isolated product was obtained with traces of acetate, which were removed after repeated freeze-drying. HPLC: *t*_R = 7.78 min; m.p. > 280 °C (decomp.); ¹H NMR (300 MHz; [D₆]DMSO/D₂O, 1:1): δ = 6.37 (s, 1H; H₄), 7.41 (ddd, ³J(H-H) = 7.0, 8.0 Hz, ⁴J(H-P) = 3.6 Hz, 1H; H₇), 7.49 (d, ³J(H-H) = 7.9 Hz, 1H; H₆), 7.63 ppm (dd, ³J(H-H) = 7.0 Hz, ³J(H-P) = 11.7 Hz, 1H; H₅); ¹³C NMR (125 MHz; [D₆]DMSO/D₂O, 1:1) δ = 103.7 (C4), 103.9 (d, ¹J(C-P) = 171.2 Hz, C1), 117.2 (C6), 128.0 (d, ²J(C-P) =

6.8 Hz, C8), 128.8 (d, $^3J(\text{C-P})=15.0$ Hz, C7), 133.2 (d, $^2J(\text{C-P})=5.38$ Hz, C14), 138.1 (d, $^1J(\text{C-P})=170.2$ Hz, C9), 141.5 (d, $^3J(\text{C-P})=11.8$ Hz, C13), 146.2 (d, $^2J(\text{C-P})=5.6$ Hz, C2), 148.0 (d, $^2J(\text{C-P})=4.5$ Hz, C11), 149.6 (d, $^3J(\text{C-P})=12.8$ Hz, C12), 181.3 ppm (d, $^3J(\text{C-P})=15$ Hz, C3); ^{31}P NMR (121 MHz; $[\text{D}_6]\text{DMSO}/\text{D}_2\text{O}$): $\delta=9.87$, 7.18 ppm (s, $\text{PO}(\text{OH})_2$); IR (KBr) $\tilde{\nu}=960$ –1200, 1120–1220 ($\text{RPO}(\text{OH})_2$), 1530–1700 (iminoquinone), 3030–3400 (NH_2) cm^{-1} ; UV/Vis (phosphate buffer, pH 7.4): $\lambda_{\text{max}}(\epsilon)=241$, 452 nm (8800); MS (ESI) m/z (%): 370.96 (100) $[\text{M-H}]^-$, 392.97 (40) $[\text{M}-2\text{H}+\text{Na}]$, 290.95 (55), 273.06 (30), 220.20 (60), 78.84 (30); HRMS (ESI, $-ve$ mode) calcd for $\text{C}_{12}\text{H}_9\text{N}_2\text{O}_8\text{P}_2$: 370.9834, found: 370.9854.

Acknowledgements

This research was supported in part by the European Commission, Sixth Framework Program (NMP2-CT2004-505899, SOPHIED) and in part by the UCL, Belgium Concerted Research Programme ARC 08/13-009. J.M.-B. is a senior research associate of FRS (FNRS, Belgium). Investigations at the CELL Unit were supported by FNRS, Région wallonne, Région bruxelloise, Loterie nationale, Concerted Research Actions and Interuniversity Attraction Poles.

Keywords: biocatalysis · dyes/pigments · endocytosis · fluorescent probes · lysosomes

- [1] L. D. Lavis, R. T. Raines, *ACS Chem. Biol.* **2008**, *3*, 142–155.
 [2] M. S. T. Goncalves, *Chem. Rev.* **2009**, *109*, 190–212.
 [3] R. Reents, M. Wagner, S. Schlummer, J. Kuhlmann, H. Waldmann, *ChemBioChem* **2005**, *6*, 86–94.
 [4] X. Nan, A. M. Tonary, A. Stalow, X. S. Xie, J. P. Pezacki, *ChemBioChem* **2006**, *7*, 1895–1897.
 [5] a) S. D. Conner, S. L. Schmid, *Nature* **2003**, *422*, 37–44; b) S. Mayor, R. E. Pagano, *Nat. Rev. Mol. Cell Biol.* **2007**, *8*, 603–612.
 [6] H.-L. Lee, E. A. Dubikovskaya, H. Hwang, A. N. Semyonov, H. Wang, L. R. Jones, R. J. Twieg, W. E. Moerner, P. A. Wender, *J. Am. Chem. Soc.* **2008**, *130*, 9364–9370.
 [7] P. Cupers, A. Veithen, A. Kiss, P. Baudhuin, P. J. Courtoy, *J. Cell Biol.* **1994**, *127*, 725–735.
 [8] R. Bianchini, G. Catelani, R. Ceconi, F. D'Andrea, L. Guazzelli, J. Isaad, M. Rolla, *Eur. J. Org. Chem.* **2008**, 444–454.
 [9] S. Niu, G. Ulrich, R. Ziesel, A. Kiss, P. Renard, A. Romieu, *Org. Lett.* **2009**, *11*, 2049–2052.
 [10] a) J. Jose, Y. Ueno, K. Burgess, *Chem. Eur. J.* **2009**, *15*, 418–423; b) V. Frade, M. S. T. Goncalves, J. Moura, *Tetrahedron Lett.* **2006**, *47*, 8567–8570.
 [11] V. P. Boyarskiy, V. Belov, R. Medda, B. Hein, M. Bossi, S. W. Hell, *Chem. Eur. J.* **2008**, *14*, 1784–1792.
 [12] a) N.-H. Ho, R. Weissleder, C.-H. Tung, *Tetrahedron* **2006**, *62*, 578–585; b) J. Jose, K. Burgess, *Tetrahedron* **2006**, *62*, 11021–11037.
 [13] G. W. K. Cavill, P. S. Clezy, J. R. Tetaz, R. L. Werner, *Tetrahedron* **1959**, *5*, 275–280.
 [14] a) G. L. Newton, J. R. Milligan, *Radiat. Phys. Chem.* **2006**, *75*, 473–478; b) A. Butenandt, *Justus Liebigs Ann. Chem.* **1957**, *602*, 72–79.
 [15] a) F. Bruyneel, E. Enaud, L. Billottet, S. Vanhulle, J. Marchand-Brynaert, *Eur. J. Org. Chem.* **2008**, 72–79; b) F. Bruyneel, O. Payen, A. Rescigno, B. Tinant, J. Marchand-Brynaert, *Chem. Eur. J.* **2009**, *15*, 8283–8295.
 [16] P. Savignac, B. Iorga, *Modern Phosphonate Chemistry*, CRC, Boca Raton, **2003**, p. 530.
 [17] I. Bonnaventure, A. B. Charette, *J. Org. Chem.* **2008**, *73*, 6330–6340.
 [18] A. Macchiariulo, R. Pellicciari, *J. Mol. Graph. Modell.* **2007**, *26*, 728–739.
 [19] W. W. Stewart, *Cell* **1978**, *14*, 741–759.
 [20] a) J. M. Oh, S. J. Choi, S. T. Kim, J. H. Choy, *Bioconjugate Chem.* **2006**, *17*, 1411–1417; b) X. Zhang, Y. Jin, M. R. Plummer, S. Pooyan, S. Gunaseelan, P. J. Sinko, *Mol. Pharmaceutics* **2009**, *6*, 836–848.
 [21] a) I. P. Chang, K. C. Hwang, C.-S. Chiang, *J. Am. Chem. Soc.* **2008**, *130*, 15476–15481; b) A. Vertut-Doi, S. Onishi, J. Bolard, *Antimicrob. Agents Chemother.* **1994**, *38*, 2373–2379.
 [22] M. Marsh, *Endocytosis, Frontiers in Molecular Biology*, Oxford University Press, **2001**, p. 283.
 [23] M. Mettlen, A. Platek, P. Van Der Smissen, S. Carpentier, M. Amyere, L. Lanzetti, P. de Diesbach, D. Tyteca, P. J. Courtoy, *Traffic* **2006**, *7*, 589–603.
 [24] P. de Diesbach, F. N'Kuli, C. Berens, E. Sonveaux, M. Monsigny, A. C. Roche, P. J. Courtoy, *Nucleic Acids Res.* **2002**, *30*, 1512–1521.
 [25] N. G. Lipsky, R. E. Pagano, *Science* **1985**, *228*, 745–747.
 [26] a) J. Yin, A. J. Lin, P. D. Buckett, M. Wessling-Resnick, D. E. Golan, C. T. Walsh, *Chem. Biol.* **2005**, *12*, 999–1006; b) K. D. Bellve, D. Leonard, C. Standley, L. M. Lifshitz, R. A. Tuft, A. Hayakawa, S. Corvera, K. E. Fogarty, *J. Biol. Chem.* **2006**, *281*, 16139–16146.
 [27] H. E. Gottlieb, V. Kotlyar, A. Nudelman, *J. Org. Chem.* **1997**, *62*, 7512–7515.
 [28] E. Wiame, D. Tyteca, N. Pierrot, F. Collard, M. Amyere, G. Noël, J. Desmedt, M. C. Nassogne, M. Vikkula, J. N. Octave, M. F. Vincent, P. J. Courtoy, E. Boltshauser, E. Van Schaftingen, *Biochem. J.* **2010**, *425*, 127–136.

Received: March 6, 2010

Published online on June 8, 2010